Neonatal hydrocephalus is a result of a block in folate handling and metabolism involving 10 formyl tetrahydrofolate dehydrogenase.

DOI:
10.1111/jnc.13686

Document Version
Accepted author manuscript

Journal of Neurochemistry JNC

Neonatal hydrocephalus is a result of a block in folate handling and metabolism involving 10 formyl tetrahydrofolate dehydrogenase.

Journal:	*Journal of Neurochemistry*
Manuscript ID	JNC-2015-1028.R3
Manuscript Type:	Original Article
Date Submitted by the Author:	29-Apr-2016
Complete List of Authors:	Naz, Naila; University of Manchester, life sciences Jimenez, Alicia; University of Manchester Vilaplana, Anna ; Hospital Ramón Y Cajal, Servicio de Bioquimica-Investigacion, Madrid, Spain Gurney, Megan; University of Manchester, life sciences Miyan, Jaleel; The University of Manchester, Faculty of Life Sciences
Area/Section:	Molecular Basis of Disease
Keywords:	Folate, FDH, Hydrocephalus, Nucleus, FR alpha, Brain, Liver

Neonatal hydrocephalus is a result of a block in folate handling and metabolism involving 10 formyl tetrahydrofolate dehydrogenase.

Naila Naz*, Alicia Requena Jimenez, Anna Sanjuan-Vilaplana, Megan Gurney, Jaleel Miyan.

Faculty of Life Sciences, The University of Manchester, 3.540 Stopford Building, Oxford Road, Manchester M13 9PT, United Kingdom.

***Author for correspondence:**

Dr Naila Naz
Faculty of Life Sciences
The University of Manchester
3.540 Stopford Building
Oxford Road
Manchester. M13 9PT
Naila.naz@manchester.ac.uk
+44 161 275 8579

Running Title:

A fault in FDH exists in neonatal hydrocephalus.

Abstract

Folate is vital in a range of biological processes and folate deficiency is associated with neurodevelopmental disorders such as neural tube defects and hydrocephalus. 10-formyl-tetrahydrofolate-dehydrogenase (FDH) is a key regulator for folate availability and metabolic interconversion for the supply of 1-carbon groups. In previous studies we found a deficiency of FDH in CSF associated with the developmental deficit in congenital and neonatal hydrocephalus. In the present study, we therefore aimed to investigate the role of FDH in folate transport and metabolism during the brain development of the congenital hydrocephalic (H-Tx) rat and normal (Sprague dawley) rats. We show that at embryonic (E) stage E18 and E20, FDH positive cells and/or vesicles derived from the cortex can bind methyl-folate similarly to folate receptor alpha, the main folate transporter. Hydrocephalic rats expressed diminished nuclear FDH in both liver and brain at all postnatal (P) ages tested (P5, P15 and P20) together with a parallel increase in hepatic nuclear methyl-folate at P5 and cerebral methyl-folate at P15 and P20. A similar relationship was found between FDH and 5-methyl cytosine, the main marker for DNA methylation. The data indicated that FDH binds and transports methyl-folate in the brain and that decreased liver and brain nuclear expression of FDH is linked with decreased DNA methylation which could be a key factor in the developmental deficits associated with congenital and neonatal HC.

Key words: Folate, FDH, Hydrocephalus, Nucleus, FR alpha, Brain, Liver

Introduction

Hydrocephalus (HC) is clinically defined as accumulation of CSF in the ventricles and spaces around the brain, usually accompanied with raised intracranial pressure in the postnatal period, due to an imbalance in CSF production and absorption, most usually a problem in CSF drainage. Nevertheless the developmental deficiencies observed have been attributed to widespread areas of brain in addition to the periventricular white matter, with no general anomalies in the fetus, and the possibility of apparently normal intellectual function if treated soon after birth (Lewin 1980). Fetal HC is a major cause of termination of unborn babies around the world yet still accounts for 1:500 live human births globally according to the NIH. In order to understand better the causes and etiology of fetal hydrocephalus, the best experimental model has proven to be the hydrocephalic Texas (H-Tx) rat (Kohn *et al.* 1981), which recapitulates the clinical signs and symptoms of human congenital hydrocephalus in many aspects. These rats have inherent vulnerability to develop this condition from late gestation (Jones and Bucknall 1988;Mashayekhi *et al.* 2002;Pourghasem *et al.* 2001) in the main phase of development of the cerebral cortex. None are "normal" so that they are classified as unaffected (UH-Tx) or affected (AH-Tx) depending on gross head shape, cortical tissue development and ventricular size. Previous studies linked fetal-onset hydrocephalus to a specific lack of the folate binding protein and enzyme, 10-formyl tetrahydrofolate dehydrogenase (FDH), also known as aldehyde dehydrogenase, ALDH1L1, in CSF (Cains et al. 2009). Significantly both affected and unaffected H-Tx fetuses respond positively to natural folates given as maternal supplements but not to folic acid which precipitated higher numbers of affected pups in the H-Tx rats and is suspected to block folate transport across the choroid plexus (Cains et al. 2009).

Within the cell, folate is present in different interconvertible forms through a series of complex reactions carried out by a range of enzymes (Kisliuk 1999;Wagner 2001), one of these is FDH. FDH is central to folate metabolism and is highly expressed in liver, the main site of folate metabolism (Krupenko and Oleinik 2002), as well as in the brain. Studies reported that mice lacking FDH had decreased folate levels indicating the importance of the enzyme in maintaining folate levels and in balancing folate metabolism (Champion et al. 1994). A significant reduction in reproductive ability of these mice was also reported (Giometti et al. 1994) indicating that disturbance of the FDH gene has widespread physiological consequences. Although the exact biological role of FDH is not clearly established yet, this enzyme appears to be a critical controller of cellular metabolism in general as well as acting as a folate binding protein, buffering folate concentrations and also transporting folate to different locations in and around the cell (Krupenko 2009). In the brain we have found that FDH is secreted into the CSF and appears to transport folate through the fluid system to supply downstream areas of the brain (Cains *et al.* 2009) so that it also seems to have a folate binding and transport function here but using the CSF to deliver to receiving cells rather than just within the cell. This is one aspect of the unique cerebral folate handling

system.

Folate is a rate limiting and critical vitamin for several different cellular pathways, most notably for DNA synthesis, maintenance and methylation (McKay et al. 2004;Miller et al. 2008) together with protein and lipid methylation, feeding into the transsulphuration pathway and urea cycle, and feeding biosynthetic pathways for key neurotransmitters (Lucock 2000). Correct DNA synthesis requires folate and its involvement in purine and pyrimidine synthesis. DNA methylation is necessary for normal genome regulation and development for which folate is also a key source of the one carbon group. The fact that DNA hypo-methylation can be overturned by folic acid supplementation indicates that a lack of folate alone can affect DNA methylation (Pufulete et al. 2005). Poor DNA methylation is linked with a number of diseases and neurological disorders (Urdinguio et al. 2009). Moreover, it has been reported that a deficiency of cerebral folate is linked with different neurological conditions (GORDON 2009;Hansen and Blau 2005;Ramaekers et al. 2007) including fetal hydrocephalus (Cains et al. 2009;Owen-Lynch et al. 2003) in addition to its already critical role in successful neurulation and prevention of neural tube defects (Burren et al. 2008;Burren et al. 2010;Dunlevy et al. 2006a;Dunlevy et al. 2006b;Dunlevy et al. 2007;Fleming and Copp 1998;Narisawa et al. 2012;Pai et al. 2015).

In the present study, we selected four key stages of HC; embryonic day (E) 18 (when CSF blockage and accumulation is established in the H-Tx rats), post-natal (P) 5 as early HC, P15 intermediate HC and P20 advanced HC in AH-Tx rats as categorized by Jones and colleagues (Harris *et al.* 1996;Jones and Andersohn 1998). Although previous studies used Wistar rats as controls, we have used Sprague dawley (SD) animals because they have the same gestational period as H-Tx rats and they show no obvious abnormalities in cortical development under normal conditions. We investigated these time points for temporal changes in two critical proteins for folate metabolism; FDH and folate receptor alpha (FRα_ as well as on two folates, folic acid (FA) and 5mTHF. The aim of this study was to elucidate the affinity of FDH for 5mTHF and to determine if HC is associated only with the cerebral folate deficiency we previously described (Cains et al. 2009) or if a more general fault in folate metabolism exists in the H-Tx strain and/or is restricted to affected individuals. We analyzed the expression pattern of the key folate metabolic proteins and the key folates; FA and 5mTHF to examine this in detail. We also examined methylation status using the DNA methylation reporter 5methyl cytosine.

Materials and Methods

Animal and tissue collection

All experiments were sanctioned by the Home Office Animal Procedures Inspectorate. Colonies of SD and H-Tx rats were maintained on a 12h light 12h dark cycle beginning at 8am, at constant temperature and humidity and with constant controlled and filtered air supply, low light and sound levels with free

access to food and water. The H-Tx colony was maintained through brother-sister mating between unaffected animals, and the SD colony was maintained though random pair mating. The animals were fed the standard Beekay rat and mouse diet no. 2 (B and K Universal, Hull, UK). We believe the SD rats are the best to use as controls since they have the same gestational cycle length as H-Tx rats and from our previous studies, share temporal coincidence in brain development. Time mated pregnant dams were isolated from the colony into cages of 3 dams. H-Tx fetuses at E18 were classified as either affected A-HTx or unaffected U-HTx based on the excessive CSF accumulation which showed as a gross dooming of the head of affected individuals under Leica MZ6 microscope (Switzerland). Furthermore, brain slices were observed under the microscope and thick slices of cortex demonstrated enlarged ventricles and thin or reduced cortical mantle thickness. In this study we found that the folate error was independent of severity of hydrocephalus and that there was a clear distinction between affected and unaffected brains therefore for the purposes of this analysis we did not correlate our findings with severity but this may be important for subsequent studies. Pregnant dams (at least 3 to 5 in each group) were euthanized by intraperitoneal injection of sodium Pentobarbitone 20% w/v (Pentoject, UK) and fetuses harvested at E 18. Pups (at least 3 to 5 in each group) were euthanized in the same way to harvest liver and brain at P5, P15 and P20. Organs were removed and immediately frozen with dry ice-cooled isopentane (VWR International S.A.S, France) and stored at -80^{0}C.

Immunohistochemistry

Immunohistochemistry was performed on 15-20 µm thick coronal and sagittal brain cryosections collected onto glass slides. Hematoxylin and eosin (H&E) staining was performed to demonstrate changes in ventricular size and cortical thickness. Double or single immunofluorescence staining was performed to show the localization of FDH, FRα and 5mTHF. After fixation for 10 minutes in paraformaldehyde, the sections were then blocked with 5% fish gelatin for an hour at room temperature. After 3 washes for 5 minutes in PBS, sections were incubated overnight at 4^{0}C with combinations of the primary antibodies; FDH 1:5000, FRα (R&D Systems) 1:10000, 5mTHF (Sigma) 1:500, GFAP (abcam (1:500). The next day, after 3 washes for 5 minutes in PBS, sections were incubated in the dark at room temperature with the subsequent secondary antibody. The nuclei were counter stained with DAPI and sections were mounted. The negative controls were incubated in the same way with the omission of primary antibody. Photomicrographs were captured with 3DHistech Panoramic 250 Flash II slide scanner, Leica confocal and Leica DMLB fluorescence microscope connected to a Coolsnap digital camera (Princeton Scientific Instruments, Monmouth Junction, New Jersey, USA) and Metaview V7 image capture and analysis software.

ELISA

Standard curve preparation: To determine FDH affinity for 5mTHF, a custom ELISA assay was developed. A first step consisted of producing FDH standard curves utilizing an FDH ELISA

commercial kit (Cusabio Biotech CO). The same kit was used to create a second FDH standard curve using the non-commercial FDH protein used in our experiments. Commercial and non-commercial FDH were full length proteins, and their corresponding standard curves were created following the company's instructions provided in the kit. FDH top standard was used at 2 x 10^7 pg/ml and two fold serial dilutions were carried out to create the standard curves. The kit limit of detection was 10.93pg/ml. Fluorescent 5mTHF antibody was prepared using the Lightning Link Cy3 conjugation kit following the manufacturer's protocol (Novus Biologicals, USA).

FDH affinity to 5mTHF: A second ELISA was carried out in parallel to the production of FDH standard curves. FDH and 5mTHf were allowed to bind as per manufacturer instructions. 5mTHF was added at the same concentration as FDH, i.e. 2 x 10^7pg/ml. A two fold serial dilution was performed to obtain a graph representing 5mTHF –FDH binding. 5mTHF and FDH concentration values chosen for the standard curve were decided according to FDH and 5mTHF data found in the literature for CSF (Cains et al. 2009). After incubation, 5mTHF-FDH complexes were identified using our prepared fluorescent anti-5mTHF antibody.

Total Protein isolation

Total protein was isolated from liver and brain tissue of rats using RIPA buffer (Sigma, USA) with 1× Roche complete protease inhibitor cocktail (Roche, USA) added. Tissues were homogenized using a Polytron homogenizer (at 3-4 speed) and centrifuged at 13000 rpm for 20 min. The supernatant was collected into another Eppendorf tube and centrifuged again to remove any debris. All steps were carried out at 4^0C.

Fractioned protein isolation

Differential centrifugation was performed as reported previously (Paulo et al. 2013). Tissues were homogenized in fraction buffer with the polytron (at 3-4 speed) for a few seconds several times, passed through a 30G needle using a 1ml syringe and incubated for 30 minutes on ice. The nuclear pellet was extracted "spinning-dry" at 720g over 5 min. 500 µl of fractionation buffer were added to the pellet which was centrifuged at 720g over 5 min. The supernatant (S1) from the first centrifugation, was deposited into a new microcentrifuge tube and was centrifuged at 10,000g over 30 min and the resulting supernatant (S2) was deposited into a new microcentrifuge tube. The pellet, containing the mitochondrial fraction (Mit_n) was washed once adding 500 µl of fractionation buffer, dispersed with a pipette, and passed through a 30 G needle (with 30mm length) using a 1 ml syringe 10 times. Mit_n was centrifuged at 10,000g for 10 min, the buffer was removed and the pellet resuspended in Laemmli buffer (Bio-Rad, USA), dispersed with a pipette, and stored at -20°C until analysis. S2 was centrifuged at 100,000g for 1 h. The resulting supernatant, the cytosolic protein fraction (Cyt_n), was deposited into a new microcentrifuge tube and kept on ice. The pellet, membrane fraction (Mem_n), was washed once adding 500 µl of fractionation buffer, dispersed with a pipette, passed through a 30 G

needle 10 times and centrifuged again at 100,000g for 1 h. 50 µl of protease inhibitor cocktail (Roche) was added to each sample and stored at -20°C until further use.

Protein determination and Western blots

Protein concentration was determined with a Nano drop instrument (Thermo Scientific, UK). For SDS PAGE electrophoresis a concentration of 20 µg of protein was loaded into each well of 4-12% (w/v) polyacrylamide 12 well NuPAGE mini-gel (Invitrogen Novex-Life Technologies, USA) were used. Protein dry transference was carried out using the iBlot Transfer and the iBlot gel Transfer mini-gels stacks PVDF Regular (Invitrogen Novex-Life Technologies, Israel) for 7 min. The nitrocellulose membrane was stained with a few drops of Ponceau solution (Amresco, USA) for 15-30 seconds to test that the transference had been successful. The membrane was washed 2x3 min with 1x PBS.

To perform the Western blot, the membrane was blocked with 5% fish gelatine or 5% skimmed milk, 1x PBS- T for 1h at RT. The primary antibodies (Table1) were diluted with 5% fish gelatin prepared in 1x PBS plus 1%Triton X 100. Primary antibody incubation took place overnight at 4°C, and membrane incubations were performed on a rotating shaker. Details of primary antibody are: anti-mouse ALDHL1 (Novus Biologicals) 1:2000, Anti-Rabbit FDH 1:5000, Anti-sheep FRα (R&D Systems) 1:10000, Anti-mouse FRα (abcam) 1:10000, Anti-mouse 5mTHF (Sigma) 1:500, Anti-mouse folic acid (Sigma) 1:500, Anti-mouse beta actin (Cell Signaling) 1:10000. The membrane was washed 4x15 min with 1x PBS-Triton X with shaking, at room temperature. Secondary antibodies were diluted with 5% fish gelatin prepared in 1x PBS. The membrane was washed 4x15 min with 1x PBS-T and placed into plastic with a little volume of PBS-Triton X.

Dot blots

Dot blots for 5methyl cytosine, folic Acid and 5mTHF were performed to qualitatively evaluate the differential concentration of these compounds between SD and H-Tx samples, analyzed in triplicates. Each sample was diluted to a final concentration of 50µg/ml and 2µl were pipetted onto separate pre-determined locations of a nitrocellulose membrane strip and allowed to air dry. Membranes were incubated in blocking solution (5% fish gelatin in 1x PBS-T) for 1hr. Samples were washed 3x15 min with 1x PBS-T. Primary antibody (Table1) incubation was carried out overnight at 4°C. Membranes were washed and then incubated with the secondary antibody for 50 min. Primary and secondary antibodies were diluted in 5% fish gelatin prepared in 1x PBS-T. All the steps were performed on a rocking table. An ECL kit was used to expose the membrane. Results from Western and dot blots were obtained using the QuemiDoc instrument (BioRad, USA); and were recorded and analyzed using Image Lab 4.1 (Bio-Rad Laboratories, USA).

Statistical analysis

Dot blot quantification was performed using Image J software version 4.0. At least three blots were analyzed for each protein from each of at least three different samples. Fluorescence images were

captured using fixed exposure times and were analyzed for level of fluorescence using Image J 1.36 b image processing software (National Institute of Health; http:rsb.info.nih.gov/ij). At least 10 images per experimental condition were analyzed. Data were analyzed using t-test where data were normally distributed or ANOVA with GraphPad prism 6.

RESULTS

Changes in cortical thickness and ventricular sizes

Hematoxylin and eosin staining was performed to compare ventricular size and cortical thickness of brains from SD at E20, UH-Tx at E16 and AH-Tx at E20. SD animals demonstrated the thickest cortex and smallest ventricles (Fig. 1A). UH-Tx had comparatively less cortical thickness with slightly enlarged ventricles compared to SD rats (Fig. 1B). AH-Tx, had greatly enlarged ventricles and the thinnest cortex (Fig. 1C). Affected pups were identified by the domed shaped head (Fig. 1E) compared to normal pup (Figure 1D).

Identification of FDH positive vesicles

Immunofluorescence staining of SD rat brain at E20 was performed to indicate the source of FDH vesicles. Confocal imaging indicated FDH+ vesicles in the ventricular space. These vesicles appeared to be breaking off the FDH+ radial glial stem cells in the cortex (Fig. 2A). The higher magnification indicated no ependymal cells around the lining and indicated FDH+ vesicles breaking away from the cortex (Fig. 2B and 2C). Double immunofluorescence staining was performed with GFAP and FDH to identify the source of FDH positive vesicles. We could detect cells positive for both proteins in the cortex and vesicles apparently breaking off the cortex into ventricular space also demonstrated both FDH and GFAP protein expression. We could detect three types of vesicles in ventricular space; i) FDH+ vesicles, ii) GFAP positive vesicles, iii) FDH and GFAP+ vesicles (Fig. 2D and 2E).

FDH has an affinity for 5mTHF

To elucidate the interactions of FDH in brain folate transport immunofluorescence staining was carried out on embryonic day 18 brain sections. Positive staining and colocalization of FDH with 5mTHF and FRα was found in the cerebral cortex of normal (Fig. 3A and 3C) and hydrocephalic brains (Fig. 3B and 3D). FDH and FRα colocalization was also found within neuroepithelia of the striatum (NPST) and vesicle-like structures present in the lateral ventricles (Fig. 3E). The data demonstrate the colocalization of FDH and 5mTHf and a similarity of roles between FDH and FRα in transporting folate both in vesicles as well as into cells. The evidence also indicates that FRα-folate containing vesicles fuse with FDH containing vesicles possibly as part of the folate transfer function. Quantification of fluorescence staining in the cerebral cortex of these animals indicated a significant decrease in FDH protein in U-HTx rats compared to that in SD, However, both FRα and 5mTHF were found to be significantly increased in U-HTx animals (Fig. 3G; $P \leq 0.01$). This makes some sense when FDH is associated more with the

developing cortex and may be reduced as cortical development is also significantly reduced in HC (Mashayekhi *et al.* 2002;Owen-Lynch *et al.* 2003)

FDH and 5mTHF ELISA

To evaluate whether FDH binds 5mTHF a sandwich ELISA was performed. Standard curves were created in order to confirm FDH was bound to the ELISA kit solid phase using first the kit's FDH standard protein and later the non-commercial FDH (from Dr. S. Krupenco) which was used in all other experiments. The aim was to demonstrate that our non-commercial FDH behaved similarly to the commercial standard protein. Equal concentrations of FDH and 5mTHF were added to the wells in order to achieve concomitant double serial dilutions for both molecules (Fig. 4A). Estimation of amount of 5mTHF bound to FDH was achieved by using a custom fluorescent 5mTHF antibody. There was an approximately linear relationship between fluorescence and 5mTHF concentration, with r^2=0.74, demonstrating that 5mTHF does bind to FDH (Fig. 4B).

Western blot analysis

Western Blot analysis of hepatic and cerebral cortical proteins indicated an abundant expression of FDH and FR alpha in both tissues. 5 days post-natal (P5), FDH was detected in the nuclear fraction of hepatic and cortical tissue of SD rats. However, in H-Tx animals, hepatic and cortical FDH was expressed mainly in the cytoplasm and membrane with a reduced expression in mitochondria and decreased or no expression in the nucleus (Fig. 5A, 5E). Similarly, compared to SD, hepatic FRα protein was restricted to the cytoplasm of AH-Tx animals (Fig. 5B). Additionally, brain cortex did not show any nuclear FRα expression in either animal (Fig. 5F). Dot blot analysis indicated no nuclear 5mTHF or FA in SD animals. However, HT-x animals had a measurable expression for both folates in liver (Fig. 5C and 5D). In brain, both folates were restricted to the cytoplasm (Fig. 5G and 5H).

At P15, among SD, UH-Tx and AH-Tx, the maximum expression of FDH was observed in the AH-Tx. However, similar to that observed at P5, HT-x animals had a tendency of decreased FDH in hepatic and cortical FDH when compared to SD (Fig. 6A and 6E). In cortical tissues of H-Tx animals, this decrease in FDH was paralleled by an increase in nuclear expression of both folates (Fig. 6G and 6H). A weak nuclear FRα was also detected in HT-x cortical tissue (Fig. 6F).

At P20, an overall reduction in hepatic FDH was observed in AH-Tx compared to SD animals. FDH was expressed consistently in all the protein fractions from SD liver, however, diminished expression of FDH was observed in mitochondrial and nuclear fractions of AH-Tx rats (Fig. 7A). This decrease was correlated with the reduced folates levels in H-Tx animals (Fig. 7C and 7D). An interesting finding was the detection of nuclear FDH and FR alpha in cortical tissue of HT-x animals at P20 which matched the detection of nuclear folates (Fig. 7E-7H).

Dot blots analysis

Total protein extracted from liver and brain was used to perform dot blot analysis for 5mC and FDH to identify changes in DNA methylation that might be related to FDH availability. Densitometry analysis demonstrated a non-significant but direct relation of 5mC with the availability of FDH. However, in the livers of AH-Tx animals at P5, we detected more FDH with less 5mC (Fig. 8).

Discussion

Understanding the etiology and pathophysiology of fetal hydrocephalus is key to finding effective preventatives and treatments to alleviate the neurological consequences and healthcare implications on affected individuals. Over the past few years we have identified a unique cerebral folate handling system that utilizes the cerebrospinal fluid to transport and deliver folate to the developing cerebral cortex. Thus this system is also exclusive to the cerebral cortex. We have discovered that a failure in the secretion of the folate binding protein and enzyme, 10-formyl tetrahydrofolate dehydrogenase (FDH) is responsible for a failure of cells in the cortex to access the available form of folate in CSF (5mTHF) and that supplementation with either THF or 5fTHF, or both in a synergistic combination, can prevent fetal hydrocephalus and improve brain development in the H-Tx rat model. Clearly, a more thorough understanding of how folate is transported into and through the brain as well as how it is utilized in the cells could help to uncover a more effective treatment in combination with the folate supplements. Hence, this study aimed to establish which components of the folate error were unique to the cerebral cortex and which might be more generally at fault in the affected H-Tx rats. Our starting hypothesis was that the cerebral folate fault would define the hydrocephalic rat so a surprise finding was that a similar fault existed outside the brain in folate transport to the nucleus, at least in the liver of affected animals. Given that the liver is a key site of folate metabolism, this, in retrospect could have been expected. Whether there is a direct link to hydrocephalus or whether this is a separate problem needs to be determined but it is tempting to think of a consequence on folate supply to the brain from the liver.

To the best of our knowledge, this study provides the first link between FDH, FRα and 5mTHF transport. It also reports for the first time a relationship between hepatic and cerebral cortical FDH and FRα expression, folate status and DNA methylation. The aim of this study was to understand the interactions of FDH and FRα in folate transport across the brain and whether hepatic and/or cerebral cortical nuclear FDH and FRα have a role in DNA methylation which could be linked with neonatal hydrocephalus (HC). This supports and extends our previous findings of a folate imbalance in the brain of hydrocephalic individuals and makes sense of the benefits of natural folate supplementation compared to supplementation with folic acid which seems to interfere with normal folate transport and, perhaps, in the balance of folate metabolism. The study compared three groups of rats, SD normal controls, unaffected (UH-Tx) and affected (AH-Tx) H-Tx rats. SD animals have good cortical thickness and normal sized ventricles so they serve as good control animals. UH-Tx animals are not affected but neither are they

normal as they showed comparatively reduced cortical thickness compared to SD as reported previously (Cains et al. 2009). However, AH-Tx rats have the thinnest cortex and largest ventricles compared to SD and UH-Tx indicating an imbalance in cerebrospinal fluid production and drainage which results in accumulating cerebrospinal fluid and associated raised intracranial pressure in postnatal ages.

Colocalization of FDH with 5mTHF and FRα suggests that FDH and FRα are functionally related and perform a common transport function of binding and delivering 5mTHF to different areas of brain. FDH and FRα were found to be localized in vesicles alone as well as together and localized with 5mTHF in vesicles in the lateral ventricle (LV) near the choroid plexus and neuroepithelia of areas in the process of differentiation confirming a need for 5mTHF in both regions of the brain which are in the process of differentiation. Previous work also describes such vesicles (Bachy et al. 2008;Harrington et al. 2009) and our findings indicate a role for these in the transport of FDH-5mTHF and FRα-5mTHF complexes to different areas of the brain, and, moreover, coincide with the discovery of vesicles (exosomes) transporting FRα-5mTHF complexes from choroid plexus to cerebral cortex (Grapp et al. 2013) so that our study showing a link to FDH containing vesicles completes the folate transport story. Furthermore, our ELISA results also demonstrate that FDH binds 5mTHF very well even though its proposed substrate and products are 10-formyl tetrahydrofolate and tetrahydrofolate respectively (Lucock 2000). Taking into account these findings and our results concerning FDH affinity for 5mTHF, similar to that described for FRα, it seems clear that FDH is involved in the transport of 5mTHF along with FRα from the choroid plexus to the cerebral cortex through vesicles (exosomes) formed in the cerebral cortex and choroid plexus respectively and floating in CSF (Bachy et al. 2008). Indeed our findings indicate that at the extracellular level, FDH may bind and transport 5mTHF in vesicles, providing the cerebral cortex with this key folate. At the intracellular level, FDH binding to 5mTHF may have a regulatory function in that it may store/sequester 5mTHF in situations of high 5mTHF concentration. In this study we show that vesicles originating from glial cells are GFAP and FDH positive. Previous studies have shown similar vesicles to be CD133 positive confirming their stem cell origin (Marzesco et al. 2005). Our study demonstrates in addition that they contain FDH and folate too. The other FDH only positive vesicles possibly are originating from choroid plexus.

One of the remarkable findings of the current study has been the detection of FDH in the nuclei of hepatic and cerebral cortical tissue of SD rats. Previously, nuclear expression of formaldehyde dehydrogenase was reported in olfactory sensory cells of rats (Keller et al. 1990). Formaldehyde dehydrogenase and FDH both belong to oxidoreductase group of enzymes. However, not much work has been done to describe the cellular location of FDH. In the current study, the finding of nuclear FDH was matched with diminished or no nuclear folate and increased 5mC expression suggesting that folate transported into the nucleus through FDH is utilized in DNA methylation. The nuclear FDH showed a tendency of reduction in H-Tx animals with a matched increase in nuclear presence of folates and a

decrease in 5mC protein concentration indicating a possible failure of DNA methylation due a requirement of FDH even though folates were present. The data indicate that in the absence or reduction of FDH, DNA methylation is decreased and folate is increased but remains unused in the nucleus of these cells.

5mC is a methylated form of the DNA and the first byproduct of DNA methylation that may be involved in the regulation of gene transcription. A lack of nuclear FDH indicates a restricted interconversion of folate byproducts which in turn reduces the availability of this crucial vitamin, and its donor methyl group for DNA methylation. The data suggest that FDH is essential for the proper utilization of folate in DNA methylation. Bioactive folate is already known to be essential for DNA methylation(Crider et al. 2012). At P15 and P20 there is less 5mC in both hepatic and cortical cells, this may due to the maturation of post-mitotic cells and thus less need for further DNA methylation. In AH-Tx cortex there is a decrease with age no doubt associated with the cell cycle arrest and decrease in cell proliferation associated with this condition in the developing cortex (Cains et al. 2009;Owen-Lynch et al. 2003).

Apart from the difference in abundance, FRα was present in each hepatic fraction at P5 in SD rats. However, it was absent in the nuclear fraction of HTx animals and more concentrated to the cytoplasmic protein fraction. In later time points, at P15 and P20, an apparent brain nuclear expression of FRα was detected. This detection correlated with nuclear levels of folate in brain tissue which also corresponded with the intensity of FRα detected. FRα has been previously found on the plasma and nuclear membrane and within endosome (Bozard et al. 2010). Moreover, FRα was found to translocate to the nucleus in response to folate levels where it behaves as a transcriptional factor. However the mechanism of translocation remains unclear (Boshnjaku et al. 2012). Mutations in folate receptor genes can lead to cerebral folate transport deficiency (Grapp et al. 2012). Our data indicate that diminished nuclear FRα and nuclear folate in animals at P5, could be associated with a disruption in key transcriptional events. This could lead to consequences in a series of developmental delays as was reported previously (Boshnjaku et al. 2012). However, these animals also demonstrated the highest 5methyl cytocine levels in comparison to other ages studied, which could possibly be utilizing the methyl folate present in the nucleus.

Shin et al. (1976) established that following a folic acid [3H] injection, 10% of total cellular folate was identified in the cell nuclei of rats. Moreover, more than 95% of the nuclear folate was found to be polyglutamated, highlighting that nuclear folate is an important metabolic cofactor involved in DNA synthesis, possibly repair and certainly methylation (Shin Yoon et al. 1976). The mechanisms of transport, processing, and accumulation of folate into the nucleus remain elusive. It has been proposed that folates could be actively transported into the nucleus during cell division when the nuclear membrane is lost (Stover and Field 2011) capturing folate cofactors from the cytoplasm into the nucleus during each mitotic division. This would suggest that folate is already polyglutamated within the

cytoplasm and an active nuclear transport and polyglutamation is not required in these cells. Another proposed mechanism is receptor mediated transport(Stover and Field 2011) possibly through FRα or FDH as determined in the present study.

Impaired folate metabolism is likely to lead to hydrocephalus in fetal-onset hydrocephalus through a failure to generate sufficient drainage cells in the arachnoid villi and other drainage sites outside of the brain associated with the arachnoid membrane. This is indicated by the fact that hydrocephalus is not apparent until high volume CSF secretion begins in association with the start of the major phase of cortical development. Other studies which have demonstrated disruptions to ventricular zone and subventricular zones as well as to radial glial stem cells along the ventricular lining in hyh mice and H-Tx rats could not be confirmed in this study where we saw no such disruption or loss of cells into the ventricles. However, such a phenomenon would not be surprising given the importance of folate in many cellular mechanisms which may impact intercellular adhesion and cellular integrity. The fact that these stem cells contain less FDH in the hydrocephalic brain would indicate that such processes are possible and a consequence of low folate supply. Nonetheless, we have not observed ependymal denudation or disruptions to the ventricular or sub ventricular zones in our studies so are unable to relate to the studies of Rodriguez and colleagues (Guerra et al. 2010;Jimenez et al. 2009;Oliver et al. 2013;Roales-Bujan et al. 2012;Rodriguez et al. 2012;Sival et al. 2011). It is possible that the disparate colonies of H-Tx rats have changed over the hundreds of generations and that these are now specific strain differences.

The current study has confirmed a general fault in the FDH-folate system in H-Tx rats and has further demonstrated a specific fault in the transport of FDH into the nucleus of cells of the liver and developing cerebral cortex in affected animals. This study highlights the vital importance of folate for normal brain development and, together with our previous studies, the vital importance of the correct folate and transporters to prevent upsetting the fine balance in folate metabolism in the brain. Although further experiments are needed the data go a long way to explain the s-phase cell cycle arrest observed in the developing fetal hydrocephalic cerebral cortex, as well as in the developmental deficits in the cortex generally through poor DNA methylation and transcription control. What we do know is that a fault in CSF drainage, which itself may be a consequence of a cerebral folate deficiency, results in a virtual shut down of the cerebral folate handling system to effectively halt cerebral development. This may be designed to prevent potential abnormal development which inevitably leads to neurological consequences and may also lead to brain tumors, whether this is in poor DNA synthesis, DNA methylation and gene expression, or poor/abnormal development through effects on cell division and migration. What is clear is that folate is an essential component in normal brain development dependent on the transport and supply of the correct forms of folate to maintain the different processes in development. In this study we found a clear difference between affected and unaffected individuals so did not carry out correlations with severity of ventriculomegaly/hydrocephalus. What seems to be the

case is that there is some physiological switch that determines whether an individual will be hydrocephalic or unaffected. We believe this likely to be in the level of drainage insufficiency. The severity would also then be determined by the level of drainage insufficiency but would be independent of the effect on the folate supply system described here. This needs more detailed investigation since we did not carry out correlations with severity of ventriculomegaly. Wide variability in ventriculomegally is a characteristic of both experimental and clinical hydrocephalus and is one very important determining factor in treatments and outcomes in patients. Our low number of experimental animals prohibited any correlation of our data with this measure of severity so that one important follow-on study must include such a measure to determine whether the folate system is indeed independent of this or whether there are further changes we can measure associated with severity of ventriculomegally which may also impact on proposed treatment through the folate system. This would be particularly important for postnatal stages after onset of rising intracranial pressure which may be not respond to folate treatments as well, if at all compared with prenatal stages.

Acknowledgement

This study was funded by The Charles Wolfson Charitable Trust. ARJ was supported on a BBSRC doctoral scholarship as well as a separate grant from The Charles Wolfson Charitable Trust. We are thankful to Dr. S. Krupenko for a generous gift of FDH antibody used in this study as well as his valuable and intellectual discussions. We are very thankful to Mrs. Sally Ashe and Rebecca Hughes for animal care and tissue collection, and to Dr Jane-Owen-Lynch for providing access to confocal imaging at Lancaster University. The slide scanner used in this study was purchased with grants from BBSRC, The Wellcome Trust and the University of Manchester Strategic Fund. Special thanks go to Mr. Roger for his help with slide scanning.

Conflict of interest

The authors have no conflict of interest for the present study.

Reference List

Bachy I., Kozyraki R. and Wassef M. (2008) The particles of the embryonic cerebrospinal fluid: how could they influence brain development? *Brain Res. Bull.* **75,** 289-294.

Boshnjaku V., Shim K. W., Tsurubuchi T., Ichi S., Szany E. V., Xi G., Mania-Farnell B., McLone D. G., Tomita T. and Mayanil C. S. (2012) Nuclear localization of folate receptor alpha: a new role as a transcription factor. *Sci Rep* **2,** 980.

Bozard B. R., Ganapathy P. S., Duplantier J., Mysona B., Ha Y., Roon P., Smith R., Goldman I. D., Prasad P., Martin P. M., Ganapathy V. and Smith S. B. (2010) Molecular and Biochemical Characterization of Folate Transport Proteins in Retinal M++ller Cells. *Invest Ophthalmol Vis Sci* **51,** 3226-3235.

Burren K. A., Savery D., Massa V., Kok R. M., Scott J. M., Blom H. J., Copp A. J. and Greene N. D. E. (2008) Gene environment interactions in the causation of neural tube defects: folate deficiency increases susceptibility conferred by loss of Pax3 function. *Human Molecular Genetics* **17,** 3675-3685.

Burren K. A., Scott J. M., Copp A. J. and Greene N. D. E. (2010) The genetic background of the curly tail strain confers susceptibility to folate-deficiency-induced exencephaly. *Birth Defects Research Part A: Clinical and Molecular Teratology* **88,** 76-83.

Cains S., Shepherd A., Bannister C., Owen-Lynch P. J. and Miyan J. (2009) A study of the incidence of hydrocephalus and cortical development in HTx rat fetuses treated with folate supplements. *Cerebrospinal Fluid Research* **6,** S25.

Champion K. M., Cook R. J., Tollaksen S. L. and Giometti C. S. (1994) Identification of a heritable deficiency of the folate-dependent enzyme 10-formyltetrahydrofolate dehydrogenase in mice. *Proc Natl Acad Sci U S A* **91,** 11338-11342.

Crider K. S., Yang T. P., Berry R. J. and Bailey L. B. (2012) Folate and DNA Methylation: A Review of Molecular Mechanisms and the Evidence for FolateΓÇÖs Role. *Adv Nutr* **3,** 21-38.

Dunlevy L. P. E., Burren K. A., Chitty L. S., Copp A. J. and Greene N. D. E. (2006a) Excess methionine suppresses the methylation cycle and inhibits neural tube closure in mouse embryos. *FEBS Letters* **580,** 2803-2807.

Dunlevy L. P. E., Burren K. A., Mills K., Chitty L. S., Copp A. J. and Greene N. D. E. (2006b) Integrity of the methylation cycle is essential for mammalian neural tube closure. *Birth Defects Research Part A: Clinical and Molecular Teratology* **76,** 544-552.

Dunlevy L. P. E., Chitty L. S., Burren K. A., Doudney K., Stojilkovic-Mikic T., Stanier P., Scott R., Copp A. J. and Greene N. D. E. (2007) Abnormal folate metabolism in foetuses affected by neural tube defects. *Brain* **130,** 1043-

16

1049.

Fleming A. and Copp A. J. (1998) Embryonic Folate Metabolism and Mouse Neural Tube Defects. *Science* **280,** 2107-2109.

Giometti C. S., Tollaksen S. L. and Grahn D. (1994) Altered protein expression detected in the F1 offspring of male mice exposed to fission neutrons. *Mutation Research/Genetic Toxicology* **320,** 75-85.

GORDON N. E. I. L. (2009) Cerebral folate deficiency. *Developmental Medicine & Child Neurology* **51,** 180-182.

Grapp M., Just I. A., Linnankivi T., Wolf P., L++cke T., H+ñusler M., G+ñrtner J. and Steinfeld R. (2012) Molecular characterization of folate receptor 1 mutations delineates cerebral folate transport deficiency. *Brain* **135,** 2022-2031.

Grapp M., Wrede A., Schweizer M., H++wel S., Galla H. J., Snaidero N., Simons M., B++ckers J., Low P. S., Urlaub H., G+ñrtner J. and Steinfeld R. (2013) Choroid plexus transcytosis and exosome shuttling deliver folate into brain parenchyma. *Nat Commun* **4**.

Guerra M., Blazquez J. L., Peruzzo B., Pelaez B., Rodriguez S., Toranzo D., Pastor F. and Rodriguez E. M. (2010) Cell organization of the rat pars tuberalis. Evidence for open communication between pars tuberalis cells, cerebrospinal fluid and tanycytes. *Cell Tissue Res.* **339,** 359-381.

Hansen F. J. and Blau N. (2005) Cerebral folate deficiency: life-changing supplementation with folinic acid. *Molecular Genetics and Metabolism* **84,** 371-373.

Harrington M., Fonteh A., Oborina E., Liao P., Cowan R., McComb G., Chavez J., Rush J., Biringer R. and Huhmer A. (2009) The morphology and biochemistry of nanostructures provide evidence for synthesis and signaling functions in human cerebrospinal fluid. *Cerebrospinal Fluid Research* **6,** 10.

Harris N. G., Plant H. D., Briggs R. W. and Jones H. C. (1996) Metabolite changes in the cerebral cortex of treated and untreated infant hydrocephalic rats studied using in vitro 31P-NMR spectroscopy. *J. Neurochem.* **67,** 2030-2038.

Jimenez A. J., Garcia-Verdugo J. M., Gonzalez C. A., Batiz L. F., Rodriguez-Perez L. M., Paez P., Soriano-Navarro M., Roales-Bujan R., Rivera P., Rodriguez S., Rodriguez E. M. and Perez-Figares J. M. (2009) Disruption of the neurogenic niche in the subventricular zone of postnatal hydrocephalic hyh mice. *J. Neuropathol. Exp. Neurol.* **68,** 1006-1020.

Jones H. C. and Andersohn R. W. (1998) Progressive changes in cortical water and electrolyte content at three stages of rat infantile hydrocephalus and the effect of shunt treatment. *Exp. Neurol.* **154,** 126-136.

Jones H. C. and Bucknall R. M. (1988) Inherited prenatal hydrocephalus in the H-Tx rat: a morphological study. *Neuropathol. Appl. Neurobiol.* **14,** 263-274.

Kamen B. A. and Smith A. K. (2004) A review of folate receptor alpha cycling and 5-methyltetrahydrofolate accumulation with an emphasis on cell models in vitro. *Advanced Drug Delivery Reviews* **56,** 1085-1097.

Keller D. A., Heck H. D., Randall H. W. and Morgan K. T. (1990) Histochemical localization of formaldehyde dehydrogenase in the rat. *Toxicol. Appl. Pharmacol.* **106,** 311-326.

Kisliuk R. (1999) Folate Biochemistry in Relation to Antifolate Selectivity, in *Antifolate Drugs in Cancer Therapy,* (Jackman A., ed), pp. 13-36. Humana Press.

Kohn D. F., Chinookoswong N. and Chou S. M. (1981) A new model of congenital hydrocephalus in the rat. *Acta Neuropathol.* **54,** 211-218.

Krupenko S. A. (2009) FDH: an Aldehyde Dehydrogenase Fusion Enzyme in Folate Metabolism. *Chem Biol Interact* **178,** 84-93.

Krupenko S. A. and Oleinik N. V. (2002) 10-Formyltetrahydrofolate Dehydrogenase, One of the Major Folate Enzymes, Is Down-Regulated in Tumor Tissues and Possesses Suppressor Effects on Cancer Cells. *Cell Growth Differ* **13,** 227-236.

Lewin R. (1980) Is your brain really necessary? *Science* **210,** 1232-1234.

Lucock M. (2000) Folic Acid: Nutritional Biochemistry, Molecular Biology, and Role in Disease Processes.

Molecular Genetics and Metabolism **71,** 121-138.

Marzesco A. M., Janich P., Wilsch-Br+ñuninger M., Dubreuil V. +., Langenfeld K., Corbeil D. and Huttner W. B. (2005) Release of extracellular membrane particles carrying the stem cell marker prominin-1 (CD133) from neural progenitors and other epithelial cells. *Journal of Cell Science* **118,** 2849-2858.

Mashayekhi F., Draper C. E., Bannister C. M., Pourghasem M., Owen-Lynch P. J. and Miyan J. A. (2002) Deficient cortical development in the hydrocephalic Texas (H-Tx) rat: a role for CSF. *Brain* **125,** 1859-1874.

McKay J. A., Williams E. A. and Mathers J. C. (2004) Folate and DNA methylation during in utero development and aging. *Biochemical Society Transactions* **32,** 1006-1007.

Miller J. W., Borowsky A. D., Marple T. C., McGoldrick E. T., Dillard-Telm L., Young L. J. and Green R. (2008) Folate, DNA methylation, and mouse models of breast tumorigenesis. *Nutr Rev* **66,** S59-S64.

Narisawa A., Komatsuzaki S., Kikuchi A., Niihori T., Aoki Y., Fujiwara K., Tanemura M., Hata A., Suzuki Y., Relton C. L., Grinham J., Leung K. Y., Partridge D., Robinson A., Stone V., Gustavsson P., Stanier P., Copp A. J., Greene N. D. E., Tominaga T., Matsubara Y. and Kure S. (2012) Mutations in genes encoding the glycine cleavage system predispose to neural tube defects in mice and humans. *Human Molecular Genetics* **21,** 1496-1503.

Oliver C., Gonz+ílez C. s. A., Alvial G., Flores C. A., Rodr+íguez E. M. and B+ítiz L. F. (2013) Disruption of CDH2/N-Cadherin-Based Adherens Junctions Leads to Apoptosis of Ependymal Cells and Denudation of Brain Ventricular Walls. *Journal of Neuropathology & Experimental Neurology* **72,** 846-860.

Owen-Lynch P. J., Draper C. E., Mashayekhi F., Bannister C. M. and Miyan J. A. (2003) Defective cell cycle control underlies abnormal cortical development in the hydrocephalic Texas rat. *Brain* **126,** 623-631.

Pai Y. J., Leung K. Y., Savery D., Hutchin T., Prunty H., Heales S., Brosnan M. E., Brosnan J. T., Copp A. J. and Greene N. D. E. (2015) Glycine decarboxylase deficiency causes neural tube defects and features of non-ketotic hyperglycinemia in mice. *Nat Commun* **6**.

Paulo J. A., Gaun A., Kadiyala V., Ghoulidi A., Banks P. A., Conwell D. L. and Steen H. (2013) Subcellular

fractionation enhances proteome coverage of pancreatic duct cells. *Biochimica et Biophysica Acta (BBA) - Proteins and Proteomics* **1834,** 791-797.

Pourghasem M., Mashayekhi F., Bannister C. M. and Miyan J. (2001) Changes in the CSF Fluid Pathways in the Developing Rat Fetus with Early Onset Hydrocephalus. *Eur J Pediatr Surg* **11,** S10-S13.

Pufulete M., Al-Ghnaniem R., Khushal A., Appleby P., Harris N., Gout S., Emery P. W. and Sanders T. A. B. (2005) Effect of folic acid supplementation on genomic DNA methylation in patients with colorectal adenoma. *Gut* **54,** 648-653.

Ramaekers V. T., Sequeira J. M., Artuch R., Blau N., Temudo T., Ormazabal A., Pineda M., Aracil A., Roelens F., Laccone F. and Quadros E. V. (2007) Folate Receptor Autoantibodies and Spinal Fluid 5-Methyltetrahydrofolate Deficiency in Rett Syndrome. *Neuropediatrics* **38,** 179-183.

Roales-Bujan R., Paez P., Guerra M., Rodriguez S., Vio K., Ho-Plagaro A., Garcia-Bonilla M., Rodriguez-Perez L. M., Dominguez-Pinos M. D., Rodriguez E. M., Perez-Figares J. M. and Jimenez A. J. (2012) Astrocytes acquire morphological and functional characteristics of ependymal cells following disruption of ependyma in hydrocephalus. *Acta Neuropathol.* **124,** 531-546.

Rodriguez E. M., Guerra M. M., Vio K., Gonzalez C., Ortloff A., Batiz L. F., Rodriguez S., Jara M. C., Munoz R. I., Ortega E., Jaque J., Guerra F., Sival D. A., den Dunnen W. F., Jimenez A. J., Dominguez-Pinos M. D., Perez-Figares J. M., McAllister J. P. and Johanson C. (2012) A cell junction pathology of neural stem cells leads to abnormal neurogenesis and hydrocephalus. *Biol. Res.* **45,** 231-242.

Shin Yoon S., Chan C., Vidal A. J., Brody T. and Stokstad E. L. R. (1976) Subcellular localization of +¦-glutamyl carboxypeptidase and of folates. *Biochimica et Biophysica Acta (BBA) - General Subjects* **444,** 794-801.

Sival D. A., Guerra M., den Dunnen W. F., Batiz L. F., Alvial G., Castaneyra-Perdomo A. and Rodriguez E. M. (2011) Neuroependymal denudation is in progress in full-term human foetal spina bifida aperta. *Brain Pathol.* **21,** 163-179.

Stover P. J. and Field M. S. (2011) Trafficking of Intracellular Folates. *Advances in Nutrition: An International*

Review Journal **2,** 325-331.

Urdinguio R. G., Sanchez-Mut J. V. and Esteller M. (2009) Epigenetic mechanisms in neurological diseases: genes, syndromes, and therapies. *The Lancet Neurology* **8,** 1056-1072.

Wagner C. (2001) BIOCHEMICAL ROLE OF FOLATE IN CELLULAR METABOLISM*. *Clinical Research and Regulatory Affairs* **18,** 161-180.

Zhao R., Diop-Bove N., Visentin M. and Goldman I. D. (2011) Mechanisms of Membrane Transport of Folates into Cells and Across Epithelia. *Annu Rev Nutr* **31,** 10.

Figure Legends

Figure 1: Changes in ventricular size and cortical thickness in SD (E20), UH-Tx (E16), AH-Tx (E20) rats. SD rats (A) and UH-Tx rats (B) have thicker cortex and less wider ventricles compared to AH-Tx rats (C). Normal rat's head gross appearance (D). The AH-Tx rats had a doomed shaped head (E) indicating accumulation of cerebrospinal fluid. CC= cerebral cortex. V= ventricles. CP= choroid plexus. Magnification 25x Scale bar 500 µm

Figure 2: Confocal image of FDH immunofluorescence staining in SD brain cortex at embryonic day (E) 20. A) SD rat brain demonstrating FDH-positive radial glial cells (neural stem cells) naked to the CSF, as there is no ependymal lining at this stage in development, and giving off FDH-positive vesicles into the ventricular CSF. Magnification 200x scale bar 100µm. B and C) Higher magnification confocal image to show FDH-positive vesicles are breaking off from the cells lining the cortex around the ventricle (white arrows). Magnification 600x. Scale bar 50 µm. D) Double immunoflourence staining of GFAP and FDH. The results show the Colocalization of the both proteins in cells (D) and vesicles (E). Magnification 400 x scale bar 100 µm.

Figure 3: Immunolocalization of FDH, FRα and 5mTHf in cerebral cortex of SD and U-HTx rats. Immunofluorescence staining of FDH (green) and 5mTHF (red) in SD (A) and U-HTx (B) rat cerebral cortex. Immunofluorescence staining of FDH (green) and FRα (red) in SD (C) and U-HTx (D) rat cerebral cortex. Immunofluorescence staining of FDH (green) and FRα (red) in vesicles near NP (E) negative control shows no cross reactivity of antibodies (F). The right panel shows higher magnification (800x, scale bar 100 µm) of corresponding induvial staining. i.e. Aa corresponds to staining A. Bb

corresponds to B. Cc corresponds to C. Dd corresponds to D. Ee corresponds to E. (G) Data indicate the localization of these antibodies in cerebral cortex which gives yellow color when individual staining is merged. Magnification 400x. Scale bar 50µm. Fluorescence quantification of SD (white bars) and U-HTx (grey bars) rats. Data from a minimum of 6 sections from different brain were averaged and recorded as mean ±SEM for all embryos in each category, calculated from all litters. Analysis of variance revealed significant differences between the cerebral cortex of SD and Texas rats for FDH, FRα and 5mTHF at $p \leq 0.01$.

Figure 4: Custom fluorescent ELISA assay. A) Commercial and non-commercial (FDH) standard curves. Standard curves were produced by plotting optical density measurements versus commercial kit standard FDH (black line) and non-commercial standard protein (pink line). Regression coefficient (r) =0.98 and 0.85 respectively n=3. B) Study of potential FDH binding to 5mTHF was carried out using a custom fluorescent immunoassay. Fluorescent values were plotted versus 5mTHF concentration. A relative linear relationship with an r^2=0.74 demonstrated FDH affinity for 5mTHF. The intervariation and intravariation coefficient of the assay was 9.2 and 9.55 respectively. N=3

Figure 5: Changes in expression pattern of FDH, FR-alpha, 5mTHF and folic acid at P5. **Upper panel:** hepatic fractionated lysate; Western blot analysis for FDH (A) and FR- alpha (B) dot blot analysis for 5mTHF (C) and FA (D). **Lower panel**: brain protein lysate; Western blot analysis for FDH (A) and FR-alpha (B) dot blot analysis for 5mTHF (C) and FA (D). The figure is representative of three technical/experimental replicate.

Figure 6: Changes in expression pattern of FDH, FR-alpha, 5mTHF and folic acid at P15. **Upper panel:** hepatic fractionated lysate; Western blot analysis for FDH (A) and FR- alpha (B) dot blot analysis for 5mTHF (C) and FA (D). **Lower panel**: brain protein lysate; Western blot analysis for FDH (A) and FR-alpha (B) dot blot analysis for 5mTHF (C) and FA (D). The figure is representative of three technical/experimental replicate.

Figure 7: Changes in expression pattern of FDH, FR-alpha, 5mTHF and folic acid at P20. **Upper panel:** hepatic fractionated lysate; Western blot analysis for FDH (A) and FR- alpha (B) dot blot analysis for 5mTHF (C) and FA (D). **Lower panel**: brain protein lysate; Western blot analysis for FDH (A) and FR-alpha (B) dot blot analysis for 5mTHF (C) and FA (D). The figure is representative of three technical/experimental replicate.

Figure 8: Changes in expression pattern of 5 methyl cytocine (5mC) in relation to total FDH. The data

represent densitometry analysis of dot blots for 5mC and FDH using total protein from each organ at different time points. Data were analyzed with Graph pad prism 6 using t-test. Dot blot analysis of 5mC and FDH using total protein from rat liver and brain.

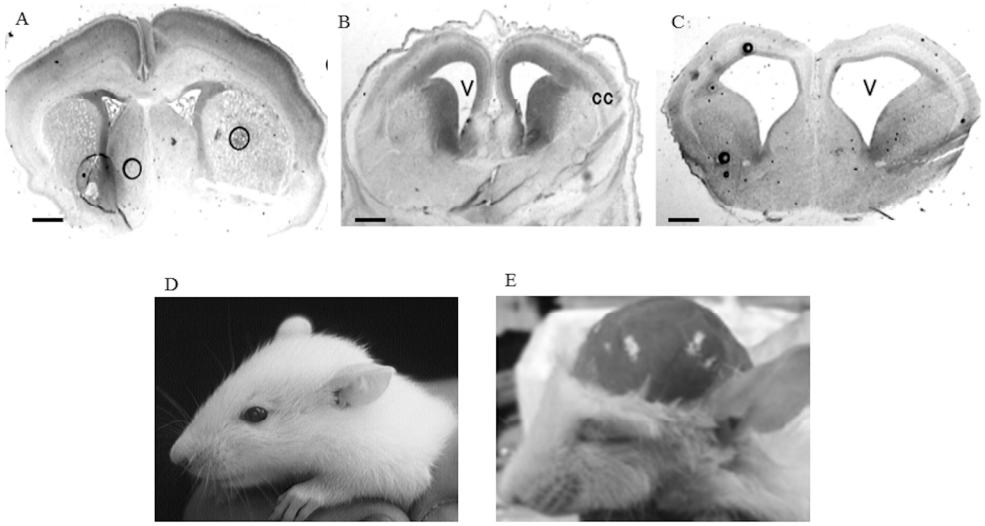

Figure 1: Changes in ventricular size and cortical thickness in SD (E20), UH-Tx (E16), AH-Tx (E20) rats. SD rats (A) and UH-Tx rats (B) have thicker cortex and less wider ventricles compared to AH-Tx rats (C). Normal rat's head gross appearance (D). The AH-Tx rats had a doomed shaped head (E) indicating accumulation of cerebrospinal fluid. CC= cerebral cortex. V= ventricles. CP= choroid plexus. Magnification 25x Scale bar 500 µm

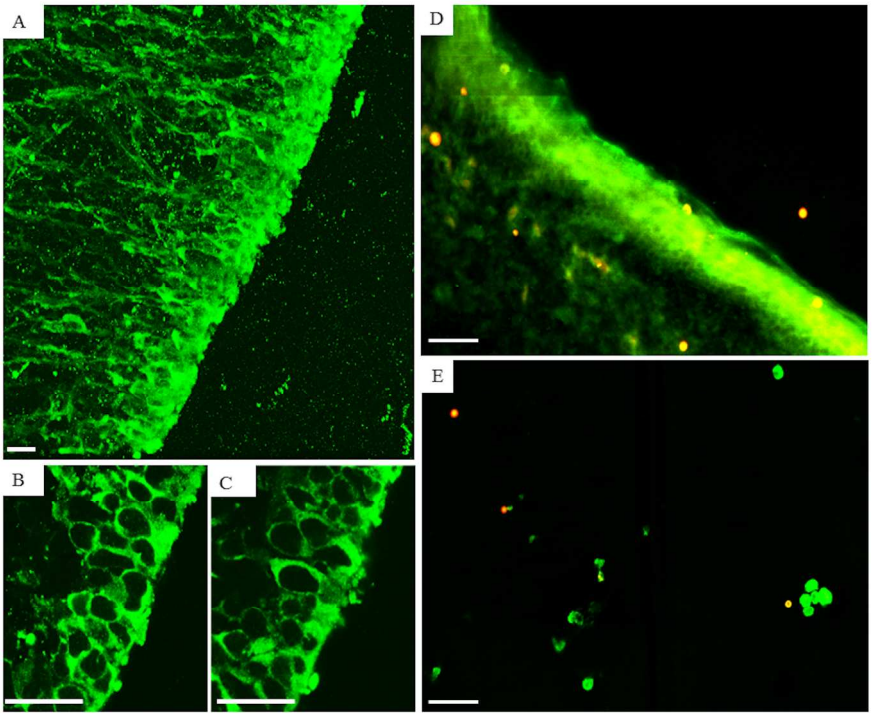

Figure 2: Confocal image of FDH immunofluorescence staining in SD brain cortex at embryonic day (E) 20. A) SD rat brain demonstrating FDH-positive radial glial cells (neural stem cells) naked to the CSF, as there is no ependymal lining at this stage in development, and giving off FDH-positive vesicles into the ventricular CSF. Magnification 200x scale bar 100μm. B and C) Higher magnification confocal image to show FDH-positive vesicles are breaking off from the cells lining the cortex around the ventricle (white arrows). Magnification 600x. Scale bar 50 μm. D) Double immunoflourence staining of GFAP and FDH. The results show the Colocalization of the both proteins in cells (D) and vesicles (E). Magnification 400 x scale bar 100 μm.

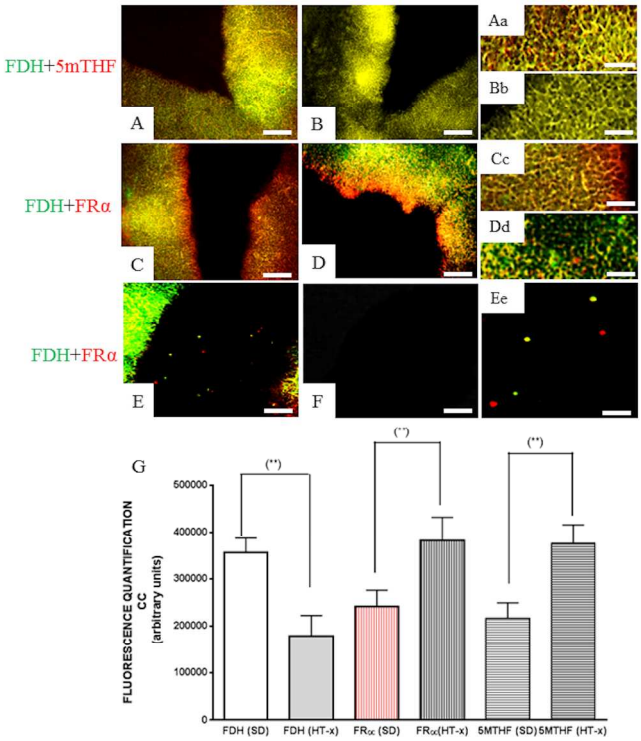

Figure 3: Immunolocalization of FDH, FRα and 5mTHf in cerebral cortex of SD and U-HTx rats. Immunofluorescence staining of FDH (green) and 5mTHF (red) in SD (A) and U-HTx (B) rat cerebral cortex. Immunofluorescence staining of FDH (green) and FRα (red) in SD (C) and U-HTx (D) rat cerebral cortex. Immunofluorescence staining of FDH (green) and FRα (red) in vesicles near NP (E) negative control shows no cross reactivity of antibodies (F). The right panel shows higher magnification (800x, scale bar 100 μm) of corresponding induvial staining. i.e. Aa corresponds to staining A. Bb corresponds to B. Cc corresponds to C. Dd corresponds to D. Ee corresponds to E. (G) Data indicates the localization of these antibodies in cerebral cortex which gives yellow color when individual staining is merged. Magnification 400x. Scale bar 50μm. Fluorescence quantification of SD (white bars) and U-HTx (grey bars) rats. Data from a minimum of 6 sections from each brain were averaged and recorded as mean ±SEM for all embryos in each category, calculated from all litters. Analysis of variance revealed significant differences between the cerebral cortex of SD and Texas rats for FDH, FRα and 5mTHF at $p \leq 0.01$.

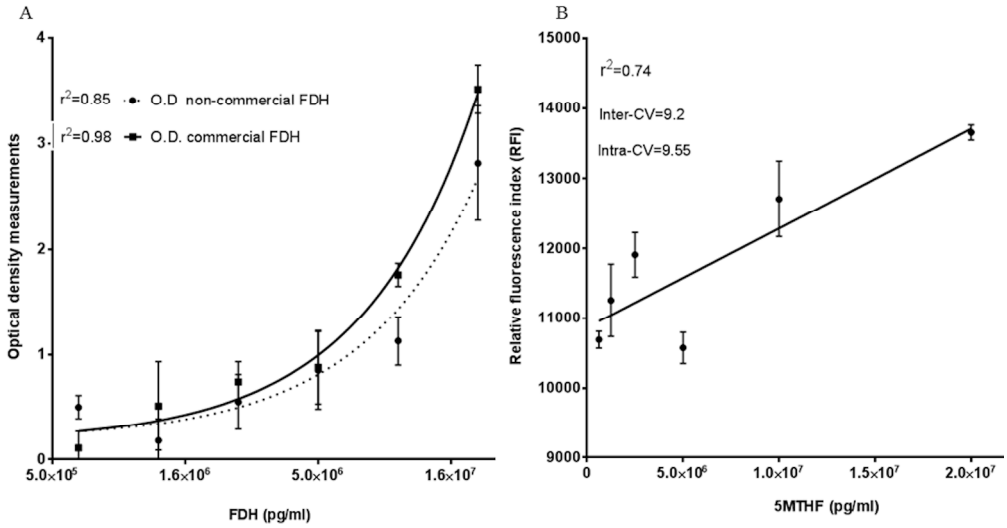

Figure 4: Custom fluorescent ELISA assay. A) Commercial and non-commercial (FDH) standard curves. Standard curves were produced by plotting optical density measurements versus commercial kit standard FDH (black line) and non-commercial standard protein (pink line). Regression coefficient (r) =0.98 and 0.85 respectively n=3. B) Study of potential FDH binding to 5mTHF was carried out using a custom fluorescent immunoassay. Fluorescent values were plotted versus 5mTHF concentration. A relative linear relationship with an r2=0.74 demonstrated FDH affinity for 5mTHF. The intervariation and intravariation coefficient of the assay was 9.2 and 9.55 respectively. N=3

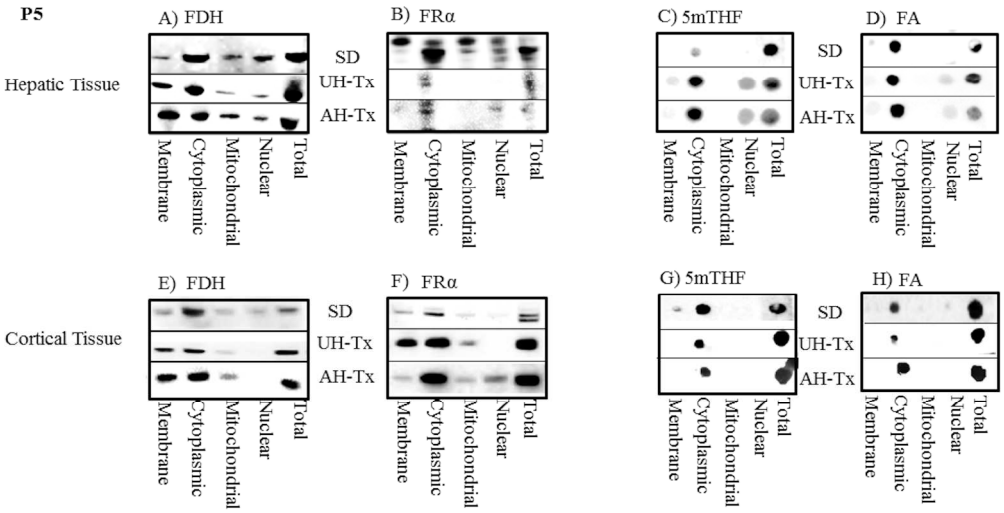

Figure 5: Changes in expression pattern of FDH, FR-alpha, 5mTHF and folic acid at P5. Upper panel: hepatic fractionated lysate; Western blot analysis for FDH (A) and FR- alpha (B) dot blot analysis for 5mTHF (C) and FA (D). Lower panel: brain protein lysate; Western blot analysis for FDH (A) and FR- alpha (B) dot blot analysis for 5mTHF (C) and FA (D). The figure is representative of three technical/experimental replicate.

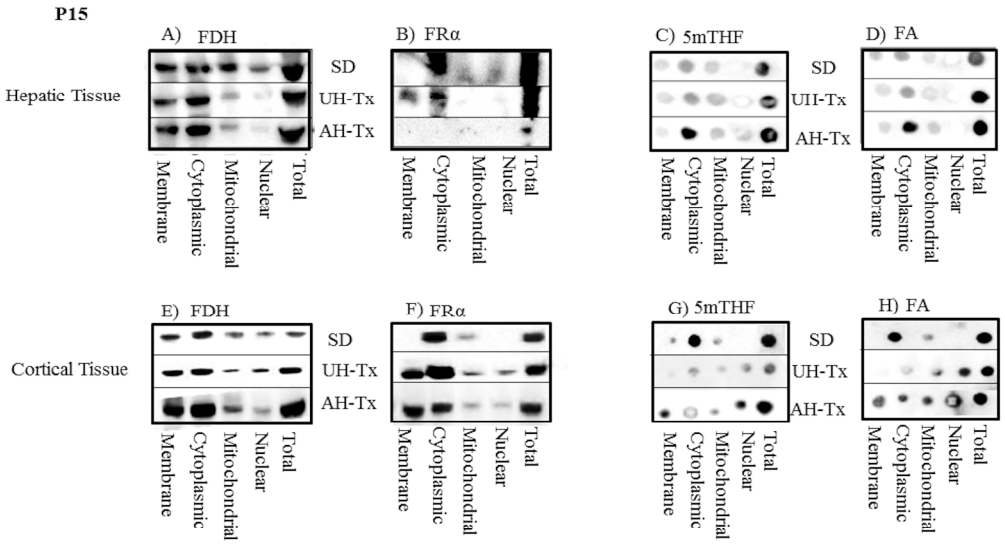

Figure 6: Changes in expression pattern of FDH, FR-alpha, 5mTHF and folic acid at P15. Upper panel: hepatic fractionated lysate; Western blot analysis for FDH (A) and FR- alpha (B) dot blot analysis for 5mTHF (C) and FA (D). Lower panel: brain protein lysate; Western blot analysis for FDH (A) and FR- alpha (B) dot blot analysis for 5mTHF (C) and FA (D). The figure is representative of three technical/experimental replicate.

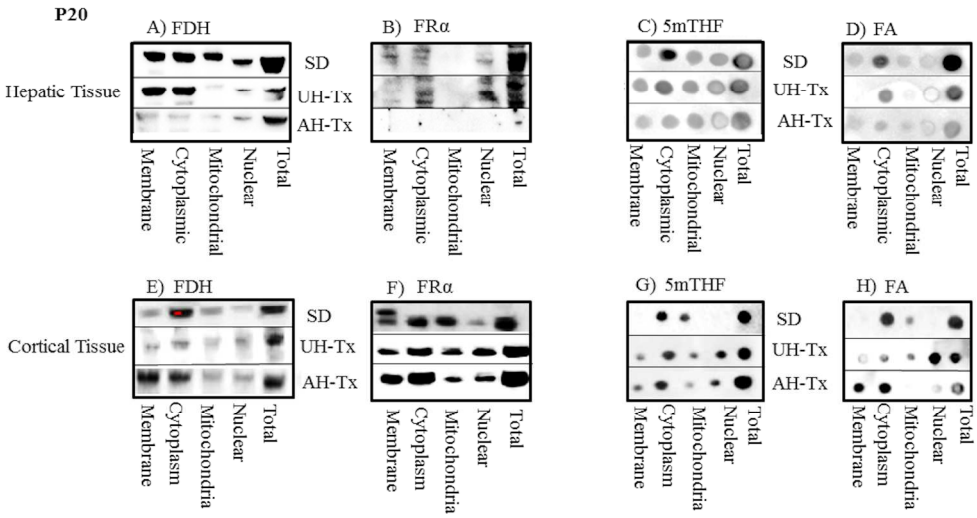

Figure 7: Changes in expression pattern of FDH, FR-alpha, 5mTHF and folic acid at P20. Upper panel: hepatic fractionated lysate; Western blot analysis for FDH (A) and FR- alpha (B) dot blot analysis for 5mTHF (C) and FA (D). Lower panel: brain protein lysate; Western blot analysis for FDH (A) and FR- alpha (B) dot blot analysis for 5mTHF (C) and FA (D). The figure is representative of three technical/experimental replicate.

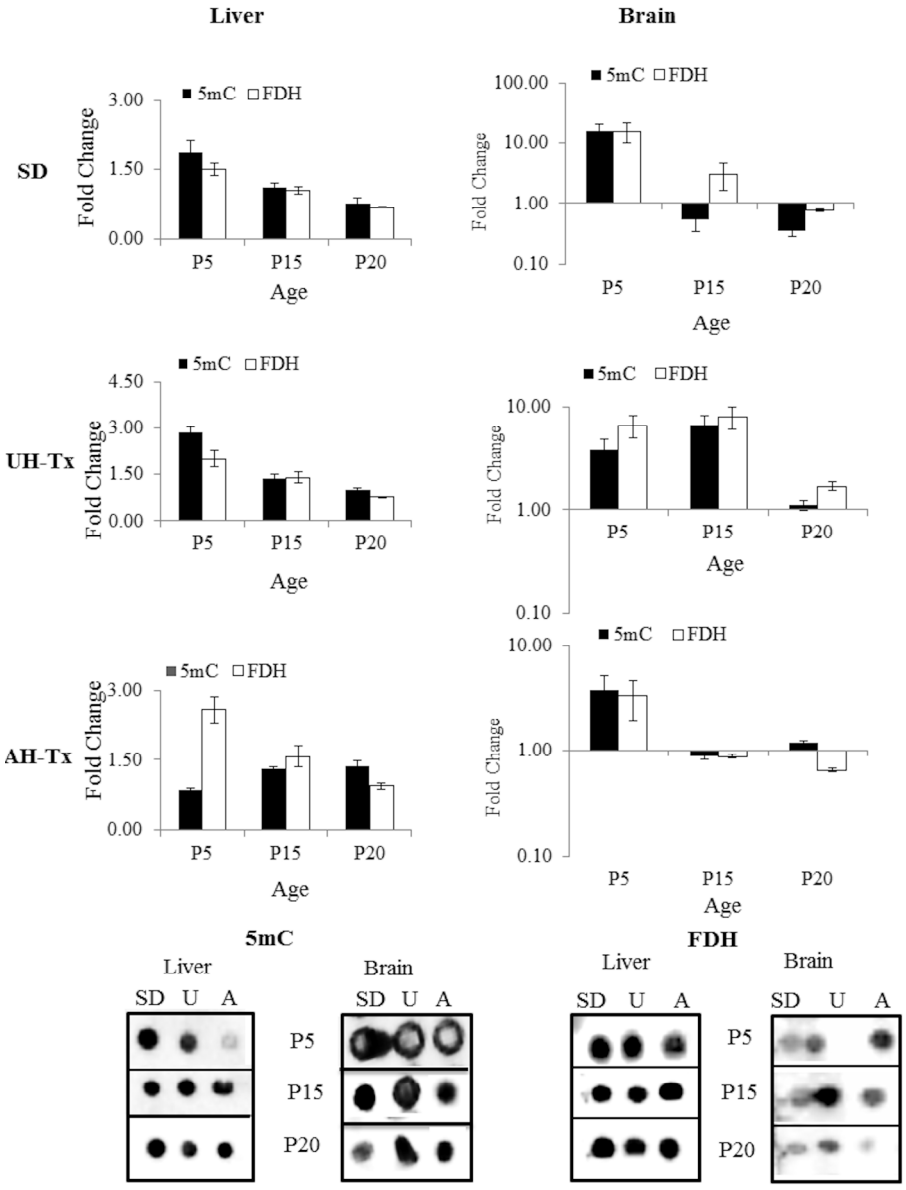

Figure 8: Changes in expression pattern of 5 methyl cytocine (5mC) in relation to total FDH. The data represents densitometry analysis of dot blots for 5mC and FDH using total protein from each organ at different time points. Data was analyzed with Graph pad prism 6 using t-test. Dot blot analysis of 5mC and FDH using total protein from rat liver and brain.

Neonatal hydrocephalus is a result of a block in folate handling and metabolism involving 10 formyl tetrahydrofolate dehydrogenase.

Naila Naz, Alicia Requena Jimenez, Anna Sanjuan-Vilaplana, Megan Gurney, Jaleel Miyan.

Supplementary results:

Subcellular localization of FDH

To confirm the subcellular localization of FDH in cerebral cortex, immunofluorescence staining of adult rat brain was performed. An intense expression of FDH was found in the nuclei of SD cortex. However, in UH-Tx rat cortex, FDH was mostly localized around the nuclei and only a few nuclei were positive for FDH which appeared in the form of small dots. AH-Tx animals showed the least or no nuclear expression for FDH (Supplementary figure 1).

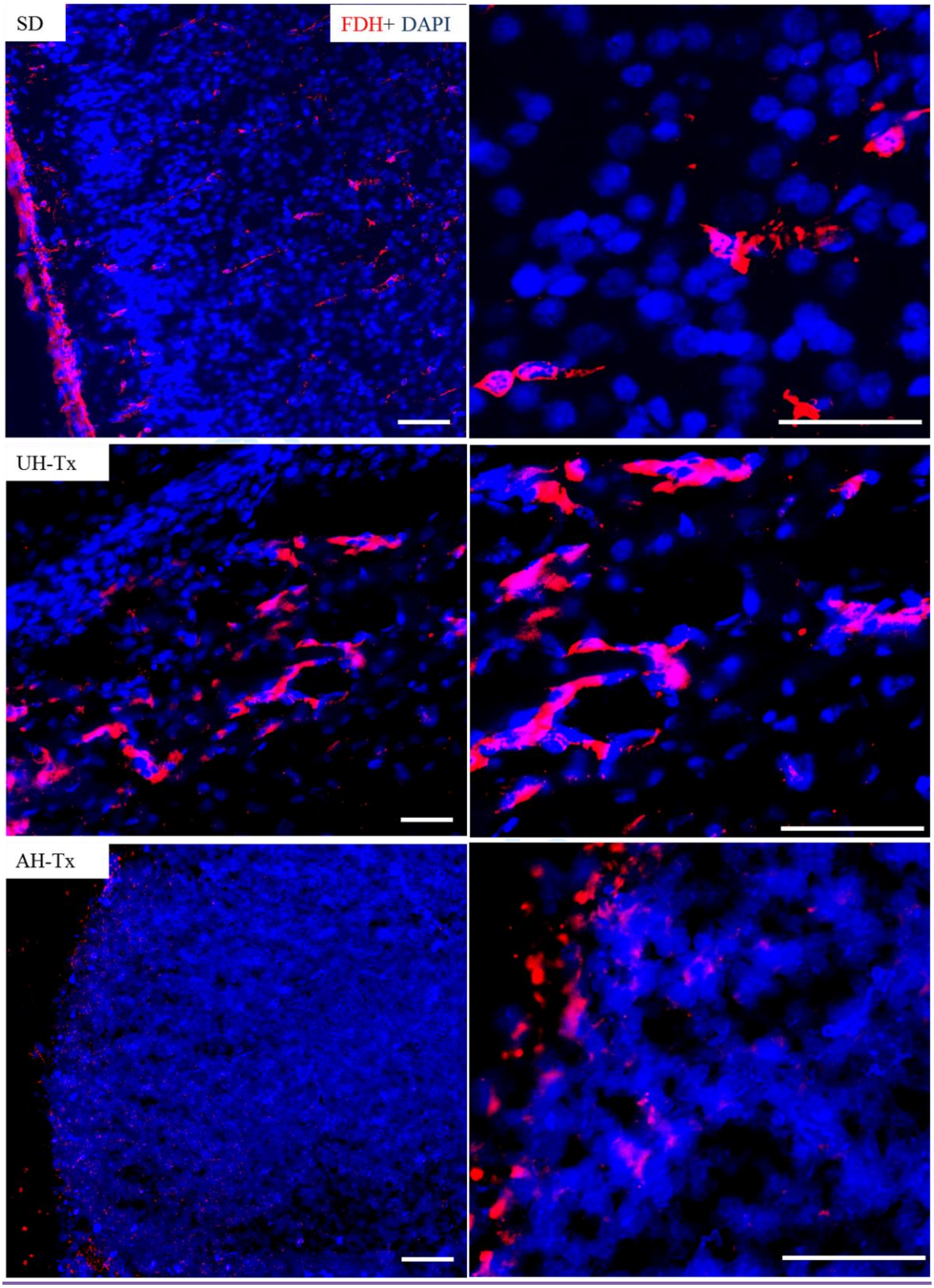

Supplementary figure 1: Immunofluorescence staining of brain cortex from SD and H-Tx animals. SD animals showed evident nuclear expression of FDH (red) localized with nuclei (blue). Left panel: magnification 200x scale bar 100µm. Right panel is higher (600x, scale bar 50 µm) magnification of left panel.

MS number	Full Paper	Date received
JNC-2015-1028.R3	Full paper	14/12/15

Special issue / comments

All authors
Naz, Naila (contact); Jimenez, Alicia; Vilaplana, Anna; Gurney, Megan; Miyan, Jaleel

Title
Neonatal hydrocephalus is a result of a block in folate handling and metabolism involving 10 formyl tetrahydrofolate dehydrogenase.

Corresponding author
Dr. Naila Naz

Address

Tel

FAX

E-mail
naila.naz@manchester.ac.uk, dr.nailanaz12@gmail.com

Date of first decision	Date received 1st revision	Date received 2nd and further revisions
03/02/16	24/02/16	2nd - 22/04/16; 3rd 29/04/16

Final Decision	Days to 1st decision	Days submission to final decision
Accepted on 23/05/16	50	109

Copyright Form	Disk Enclosed	Colour Figures
No	N/A	Yes

ISN member - Confirmation	Category
No	Molecular Basis of Disease

JNC-2015-1028.R1_InThisIssue

Folate deficiency is associated with neurodevelopmental disorders such as neural tube defects and hydrocephalus. 10-formyl-tetrahydrofolate-dehydrogenase (FDH) is a key regulator for folate availability and metabolic interconversion. We show that FDH binds and transports methyl-folate in the brain. Moreover, we found that a deficiency of FDH in the nucleus of brain and liver is linked with decreased DNA methylation which could be a key factor in the developmental deficits associated with congenital and neonatal hydrocephalus cells.